THE ABUNDANCE OF BULLET-GROUPS IN ΛCDM

J. G. Fernández-Trincado[1,2,3], J. E. Forero-Romero[1], T. Verdugo[3], G. Foëx[4] and V. Motta[4]

[1] Departamento de Física, Universidad de los Andes, Cra. 1 No. 18A-10, Edificio Ip, Bogotá, Colombia
[2] Institute Utinam, CNRS UMR6213, Université de Franche-Comté, OSU THETA de Franche-Comté-Bourgogne, Besançon, France
[3] Centro de Investigaciones de Astronomía, AP 264, Mérida 5101-A, Venezuela
[4] Departamento de Física y Astronomía, Universidad de Valparaíso, Avda. Gran Bretaña 1111, Playa Ancha, Valparaíso 2360102, Chile
Submitted for publication in ApJL

ABSTRACT

We estimate the expected distribution of displacements between the two dominant dark matter density peaks and between baryons and dark matter in halos simulated within a full cosmological context. We use as a benchmark the observation of SL2S J08544-0121, which is the lowest mass system observed so far featuring a bi-modal dark matter distribution with a dislocated baryonic component. We extend previous results by studying two halo samples: groups and clusters. We find that 50% to 60% of the dark matter halos with circular velocities in the range $300\,\mathrm{km\,s^{-1}}$ to $700\,\mathrm{km\,s^{-1}}$ (groups) show multimodal morphologies with displacements between the dark matter clumps equal or larger than $133 \pm 21 h^{-1}\mathrm{kpc}$ as observed in SL2S J08544-0121. For dark matter halos with circular velocities larger than $700\,\mathrm{km\,s^{-1}}$ (clusters) this fraction rises to 80% to 85%. Using the same simulation we estimate the dark matter-to-baryon spatial separation and find that 0.1% to 1.0% of the groups should present separations equal or larger than $87 \pm 14 h^{-1}\mathrm{kpc}$ corresponding to our observational benchmark; for clusters this fraction is in the range of 4% to 10%, consistent with previous studies of dark matter to baryon separations. The extension of the theoretical predictions and observational results towards low mass Bullet-like configurations, i.e. larger abundance of systems, opens up the possibility for a new statistical test of ΛCDM.
Subject headings: cosmology: theory – dark matter

1. INTRODUCTION

The Bullet Cluster (massive cluster of galaxies 1E0657—56) provided a new kind of observational evidence for the existence of dark matter (Markevitch et al. 2004; Clowe et al. 2006). Quantifying the displacement between dark matter and the dominant baryonic component (hot X-ray emitting gas) has been used to test the Cold Dark Matter (CDM) paradigm itself by quantifying the substructure velocity required to produce such displacement (Hayashi & White 2006; Springel & Farrar 2007; Thompson & Nagamine 2012), the displacement between the dominant dark matter and baryonic component (Forero-Romero et al. 2010) to estimate the expected abundance of such events in a ΛCDM Universe and even explore possible extensions to the concordance cosmological model (Farrar & Rosen 2007; Lee & Komatsu 2010; Lee & Baldi 2012).

Since then, other examples of Bullet-like systems have been found; MACS J0025.4-1222 (Bradač et al. 2008), Abell 2744 (Merten et al. 2011), DLSCL J0916.2+2951 (Dawson et al. 2012), ZwCl 1234.0+02916 (Dahle et al. 2013). Recently (Gastaldello et al. 2014) observed baryonic-DM displacement if 124 ± 20 kpc in a group-like system with a total mass $2.4 \pm 0.6 \times 10^{14}\mathrm{M_\odot}$. Systems of this mass are ~ 10 times more abundant than cluster systems in the mass range of the Bullet Cluster $> 10^{15}h^{-1}\mathrm{M_\odot}$, this opens up the possibility of observationally finding bullet groups in a fair amount to impose constraints on ΛCDM.

However, a greater abundance of small mass systems has to be weighted by the probability of having a merger and presenting a large displacement between the DM and baryonic components. These two conditions (merger

rates, maximum possible displacement) are a funcion of halo mass in ΛCDM cosmologies. Such study has been performed for clusters but not for lower mass systems (Forero-Romero et al. 2010). The existence of objects like SL2S J08544-0121 and observational campaigns like the Strong Lensing Legacy Survey (SL2S) open up the possibility of finding multi-modal dark matter distributions in the group mass range.

In this Letter we compute the abundance of group-like dark matter halos with a multi-modal morphology that also might present a DM-baryon displacement. To this end we use a N-body cosmological simulation with such a resolution that allows us to identify multi-modal dark matter distributions in hosts with circular velocities larger than $300\,\mathrm{km\,s^{-1}}$.

This Letter is organized as the follows. In Section 2 we present the simulation and the halo catalogs used in this work. We continue in Section 3 with the geometry of the problem at hand and the measurements setup. Next in Section 4 we present our results and observational perspectives to finally conclude in Sections 6.

2. SIMULATION, HALO CATALOGS AND PAIRS

We use the Bolshoi Run, a cosmological DM only simulation over a cubic volume of $250h^{-1}\mathrm{Mpc}$ comoving on a side. The simulation uses the ART code to follow the evolution of a dark matter density field sampled with 2048^3 from $z = 80$ to $z = 0$. The cosmology used corresponds to the spatially flat concordance model with the following parameters: the density parameter for matter (dark matter and baryons) $\Omega_m = 0.27$, the density parameter for baryonic matter $\Omega_b = 0.0469$, the density parameter for dark energy $\Omega_\Lambda = 0.73$, the Hubble pa-

rameter $h = 0.7$, the normalization of the Power spectrum $n = 0.95$ and the amplitude of mass density fluctuation (at redshift z=0) $\sigma_8 = 0.82$. These cosmological parameters are consistent with the nine-year Wilikinson Microwave Anisotropy Probe (WMAP) results (Hinshaw et al. 2013). A detailed presentation of the simulation can be found in Klypin et al. (2011).

The number of particles used for each of the DM component was 2048^3, resulting in a mass resolution of 1.35×10^8 $M_\odot h^{-1}$. The completeness limit in this simulation is set for halos with 100 particles corresponding to a mass of $1.35 \times 10^{10} h^{-1} M_\odot$ or a maximum circular velocity V_c of $50 \, \text{km s}^{-1}$.

We use halo catalogs constructed using the Bound Density Maxima (BDM) algorithm (Klypin & Holtzman 1997; Klypin et al. 1999). To define the radius of a halo we use a density threshold of 360 times the mean density of the Universe, for different redshifts we use the overdensity criterion by Bryan & Norman (1998). An important feature of BDM is that it allows us to detect sub-halos inside larger virialized structures.

All the raw data used in this Letter is available through the Multidark database [1] (Riebe et al. 2013). Furthermore, in order to facilitate the reproducibility and reuse of our results we have made available all the data and the source code available in a public repository [2].

In this Letter we make a study at four different redhifts $z = 0.0, 0.25, 0.5$ and 1.0. First, we select all the host halos (i.e. halos that are not inside a larger halo) with circular velocities $V_c \geq 300 \, \text{km s}^{-1}$. Then, we select the sub-halos with circular velocities $V_c \geq 75 \, \text{km s}^{-1}$. The objective is to use this sub-halos as the tracer of the subdominant dark matter clump in the merging cluster, i.e. the bullets.

For the redshifts $z = 0.0, 0.25, 0.5$ and 1.0 we find $10041, 10346, 10554$ and 10382 host halos and $157853, 177331, 195072, 225188$ sub-halos, respectively. These two sets (host halos and sub-halos) constitute the basis for our analysis. We find now for each host halo we its most massive sub-halo. Each pair host halo/sub-halo is considered as a potential Bullet system and is kept for the analysis described in the next Section.

3. BULLET GEOMETRY AND MEASUREMENT SETUP

The Bullet groups is composed by two halos. the host halo and the sub halo. This configuration is described by the position and velocity of the sub-halo in a frame of reference where the main halo is at rest; thus $\vec{v} = \vec{v}_{sub} - \vec{v}_{halo}$ and $\vec{r} = \vec{r}_{sub} - \vec{r}_{halo}$, where the subscripts $host$ and sub refer to the host and sub-halo in the frame of reference of the simulation, respectively.

The angle between these two vectors characterized by,

$$\mu \equiv \cos(\theta) = \frac{\vec{v} \cdot \vec{r}}{\|\vec{v}\| \, \|\vec{r}\|} \qquad (1)$$

encodes the geometry of the collision, i.e. cases of $|\mu| \approx 1$ can be considered as head-on collisions while $|\mu| \approx 0$ describe a grazing trajectory.

The bullet-like encounter can be instantaneously described by quantities the following quantities the circular

velocity of the host and the sub-halo, $V_{c,host}$ and $V_{c,sub}$; the size of the host halo R_{vir}; the relative position and velocity of the substructure, $\vec{v}$ and $\vec{r}$; and the angle between the position and velocity μ.

As a first approximation there are two quantities that are available from observations of these Bullet-like systems. The projected distance between two dominant dark matter clumps and the ratio of the galaxies luminosities associated to them. From the simulation point of view this can be translated into the 2D projected values of $\|\vec{r}\|$, its value relative to the virial radius $D_{off} = \|\vec{r}\|_{2D}/R_{vir}$ and the ratio of the circular velocities of the two clumps $V_{c,sub}/V_{c,host}$. In a higher degree of detail, in order to gain better insight we use the substructure velocity as a fraction of the host's circular velocity, $\|\vec{r}\|/V_{c,host}$, as a measure of the the strength of the interaction. Finally, we also measure the geometry of each interaction through the values for μ.

All the physical quantities described above can be used to describe the three main stages in a bullet-like encounter. First, the sub-halo crosses the virial radius of the host halo starting a head on collision, $\|\vec{r}\|/R_{vir} \approx 1$ and $\mu \approx < 0.0$. Second, as the sub-halo crosses for the first time the center of the host halo $\|\vec{r}\|/R_{vir} < 1.0$ and $\mu > 0.0$. Third, as the sub-halo reaches apogee and comes back to the center of the halo $\|\vec{r}\|/R_{vir} < 1.0$ and $\mu < 0.0$. We use this quantities in Section XXX to fully characterize the different kind of interactions observed in the Bolshoi simulation.

4. RESULTS

4.1. *Displacements and Relative Circular Velocities*

The main result of this paper is summarized in Figure 1, it presents the integrated probability distribution for the displacement between the center of the host halo and its dominant sub-halo. The left panel shows the displacement in physical units and the right panel as a fraction of the virial radius of the host halo.

Figure 1 shows the results for two different populations; groups with $300 \, \text{km s}^{-1} < V_{c,host} < 700 \, \text{km s}^{-1}$ and clusters with $V_{c,host} > 700 \, \text{km s}^{-1}$. Additionally, this is presented for all redshifts $z = 0.0, 0.25, 0.5$ and 1.0.

The panel with the physical displacements also shows a vertical stripe with the estimated displacement for the Bullet-group reported by Gastaldello et al. (2014). Considering this system as consistent withe the groups sample we see that a fraction of $\sim 15 \pm 2\%$ of the groups should present a displacement equal or larger than the one estimated for SL2S J08544-0121, this fraction is close to $45 \pm 2\%$. The panel with the normalized displacements shows a distribution that can be considered close to universal in the sense that the two samples (groups and clusters) at all redshifts present a similar trend.[...]

Figure 2 shows 2D histograms in a plane composed by the ratio of the two circular velocities $V_{c,sub}/V_{c,host}$ and the physical displacements. This is revealing because these two quantities can be constrained by observations. The displacement is a direct observable, while the ratio of the circular velocities can be estimated from lensing studies or approximated by the ratio of the total galaxy luminosity associated with the galaxy peaks.

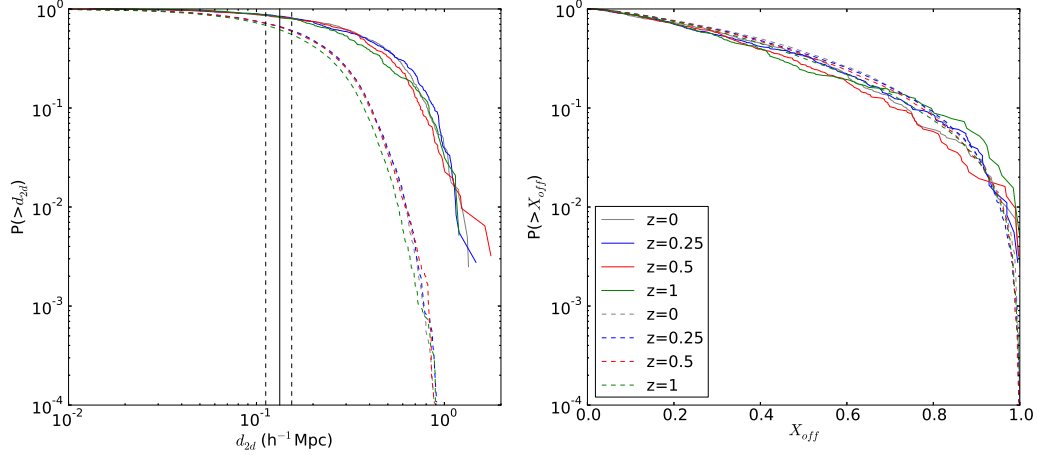To construct this figure we co-add all the halos in the

FIG. 1.— Integrated probability distribution for the displacement between the host halo and its largest sub-halo. The left panel shows the results in terms of the physical displacements while the right panel shows the displacements normalized by the virial radius of the host halo. The continuous line corresponds to the halos in the group sample $V_{\mathrm{circ,host}} > 700\,\mathrm{km\,s^{-1}}$ and the dashed lines to the sample $V_{\mathrm{circ,host}} < 700\,\mathrm{km\,s^{-1}}$. The vertical lines corresponds to mean estimate separation between the two dark matter clumps in the results reported by Gastaldello et al. (2014) for the group SL2S J08544-0121. Between 50% to 60% of the groups show a displacement equal or larger than this observational benchmark.
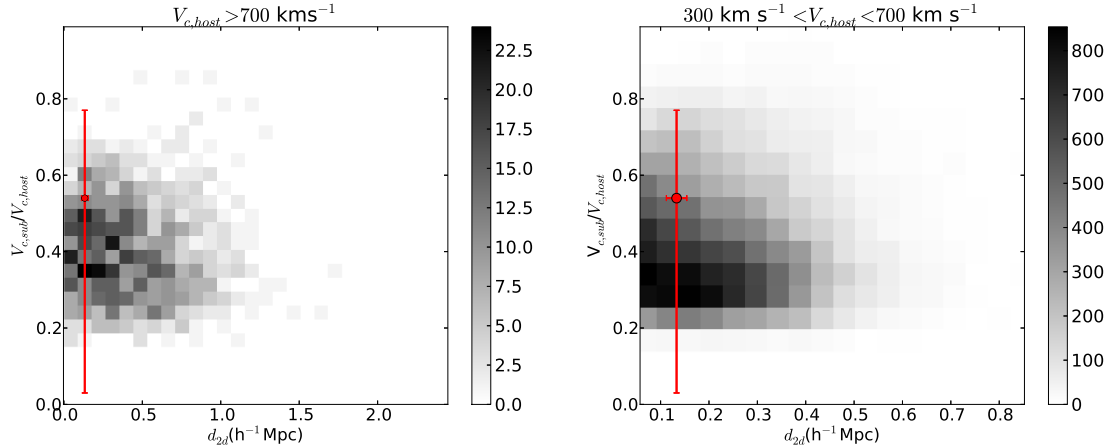

FIG. 2.— 2D histogram in the plane $V_{\mathrm{c,sub}}/V_{\mathrm{c,host}}$-$d_{2D}$. The left panel corresponds to clusters and the right panel to groups. The circle with error bars corresponds to SL2S J08544-0121 data reported from Muñoz et al. (2013) and Gastaldello et al. (2014). The data used to construct the histograms integrates the objects at all redshifts.

sample (left, groups; right, clusters) at all redshifts. We stack the data because we do not observe any strong time evolution, additionally this allows us to increase the signal in each bin. Overplotted there is an circle with error bars that represents the observational estimates for the system SL2S J08544-0121 using the fraction in velocity dispersion in the line-of-sigth of the group SL2S SJ08544-0121 ($\sigma_{host} = 341^{+43}_{-109}\,\mathrm{km\,s^{-1}}$ and $\sigma_{sub} = 185^{+30}_{-62}\,\mathrm{km\,s^{-1}}$) reported by Muñoz et al. (2013) and the DM displacement inferred from the data presented by Gastaldello et al. (2014).

4.2. *Relative Velocities*

In Figure 3 we present the integrated probability of the relative peculiar velocities of the sub-halos with respect to the host halo. The left panel presents this velocity in physical units while the left panel presents them as a fraction of the circular velocity of the host halo.

The panel with the normalized velocities shows that the distribution of sub-halo velocities is close to universal. Regardless of the mass of the host halo and the redshift the integrated distributions lie very close to each other.

The median of this distribution is located at $v/V_{\mathrm{c,host}} = 1.1$. We also note the strong break at $v/V_{\mathrm{c,host}} = 3.0$ that is present in the data from the group sample that allows us to probe fractions on the order of 10^{-4}. This break is located close the escape velocity of $v/V_{\mathrm{c,host}}$ for dark matter halos following a NFW profile with a concentration value $c \approx 6$ (Hayashi & White 2006).
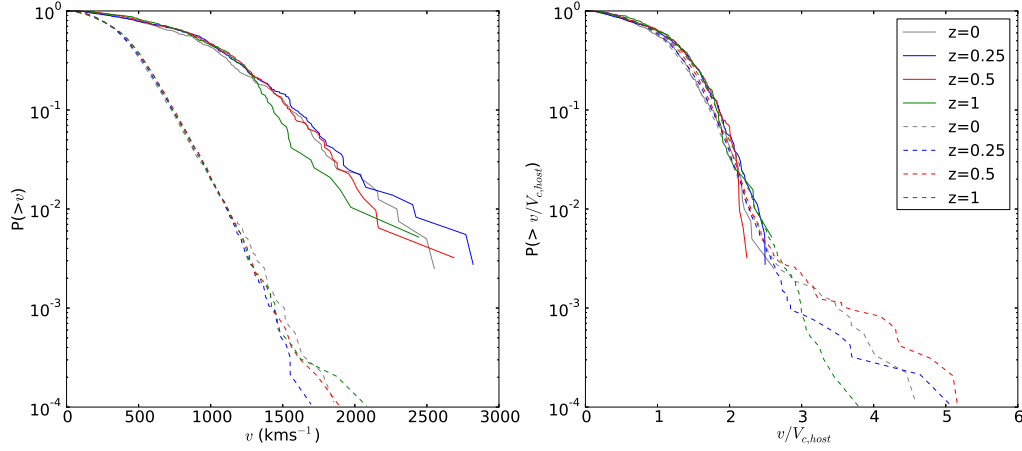
4.3. *Collision Geometries*

FIG. 3.— Integrated probability distribution for the relative velocity of the sub-halo with respect to its host. The left panel shows the results in physical units while the right panel show the same values normalized by the circular velocity of the host halo. The line coding follows the same structure as Figure 1
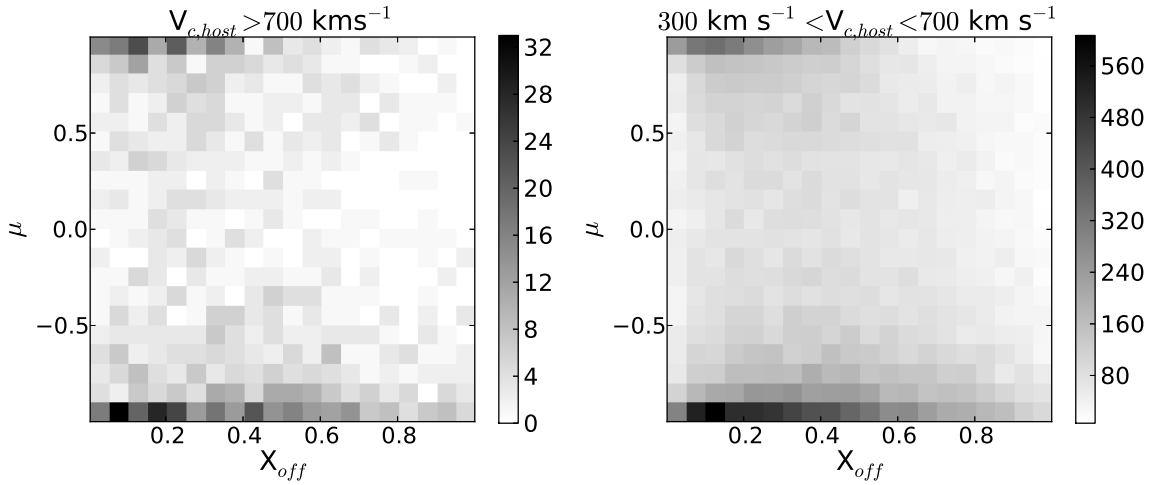

FIG. 4.— 2D histograms in the plane μ-$D_{\rm off}$. The left panel corresponds to clusters and the right panel to groups. The data used to construct this histogram includes the halos at all redshifts.

Figure 4.3 presents the geometry of the bullet groups using the variables μ and $D_{\rm off}$. The first evident feature is that most of the configurations have $|mu| > 0.9$ ($\theta \leq 30°$), meaning that most of the collisions can be described as a head-on while only a minority with $|mu| < 0.9$ have more tangential trajectories. For the pairs on radial trajectories there are three regions of interest in this plane that describe different stages in the collision, assuming that the sub-halo merges or falls below the detection threshold after the first pass through the center of the host halo.

The first region has $\mu \approx -1$ and $D_{\rm off} > 0.6$, which locates the systems where a head-on collision has just started. The sub-halo is close to the boundary of the host halo and is infalling. The second region has $\mu \approx 1$ and $D_{\rm off} < 0.6$; at this stage the collision continues after the first crossing of the host's center, the low number of

halos with radial infalling velocities and displacements $D_{\rm off} > 0.6$ suggest that this the maximum range of radii for the apogee. The third region corresponds to $\mu \approx -1$ and $D_{\rm off} < 0.6$ which corresponds to the secondary infall after apogee.

4.4. Displacement between Dark Matter and Baryons

These different collision geometries will produce different results in terms of the displacement between dark matter and baryons. Strictly speaking, the results we have derived so far, apply to multi-modal groups and their expected separation between the two dominant dark matter clumps but it should not be interpreted that all have a corresponding DM-baryon displacement. The systems where the halo is starting to fall into the host ($\mu \approx -1$, $D_{\rm off} > 0.6$) should not present a detectable DM-baryon displacement.
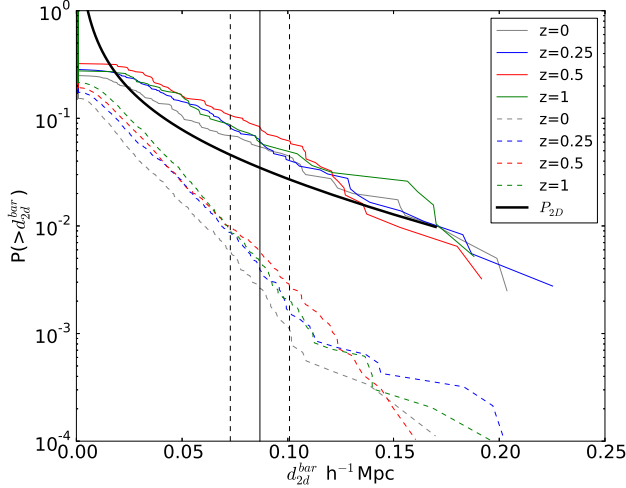
FIG. 5.— Integrated probability distribution for the estimated baryonic displacements in the group and cluster samples. The continuous line marked as P_{2D} shows the statistics reported by Forero-Romero et al. (2010) for a cosmological simulation including DM and baryons. The vertical lines correspond to the mean value and uncertainty of the displacement measured for SL2S J08544-0121.

We clearly expect such displacement in the case where the sub-structure has already passed through the center of the host halo. In this section we attempt an estimation for the DM-baryon displacement statistics. We work under the following hypothesis. First, we consider that systems with $|\mu| < 0.9$ have a baryonic displacement, $d_{2D}^{\rm bar}$, equal to zero. Second, we consider that all systems with infalling velocities $\mu < -0.9$ and large displacements $D_{\rm off} > 0.6$ also have baryonic displacements equal to zero. Third, for all the other cases we estimate the displacement between the baryons and the dominant DM peak by the distances between the dominant peak and the center of mass of the main halo, $d_{2D}^{\rm bar} = D_{\rm off} R_{\rm vir}$, where $X_{\rm off}$ is the offset computed for each host halo in the original catalog.

This simplified model does not take into account that there is a fraction of halos with $\mu < -0.9$ and $D_{\rm off} < 0.6$ for which the collision has not started and should have $d_{2D}^{\rm bar} = 0$. A detailed modeling of this fraction requires the study of the complete merger tree of the halo and sub-halo, a study beyond the scope of this Letter. Instead we caution the reader that the derived fraction of halos with a displacement $< d_{2D}^{\rm bar}$ can be considered as an upper limit.

The results for the integrated distributions for $> d_{2D}^{\rm bar}$ are shown in Figure 5. The dashed lines represented the results for groups and the continuous lines correspond

to clusters. As a test of our approach we compare the cluster results against the analytic fit provided by Forero-Romero et al. (2010). This fit reproduces the statistics for the DM-baryon separation found for clusters more massive than $> 10^{14} h^{-1} M_\odot$ in a simulation that included a description for gas with 8 times the volume of the Bolshoi Simulation. This fit is valid for separations larger than $70 h^{-1} {\rm kpc}$, beyond that separation we find that it provides a good description within a factor of ~ 2 of

5. OBSERVATIONAL IMPLICATIONS

6. CONCLUSIONS

In this Letter we estimate fraction of galaxy groups that can present observational features associated to a bullet-like event. This is motivated by the recent observational results of (Gastaldello et al. 2014) where a system (SL2S J08544-0121) on the mass range $1 \times 10^{14} h^{-1} M_\odot$ and velocity dispersion $650 \, {\rm km \, s^{-1}}$ was reported to feature a displacement between its baryonic (hot gas) and dark matter components.

Our estimate is based on large N-body dark matter only cosmological simulation. We estimate the distribution of projected displacements between the dominant DM clumps in two kinds of systems; groups with circular velocities $300 \, {\rm km \, s^{-1}} < V_{\rm c} < 700 \, {\rm km \, s^{-1}}$ and clusters with $V_{\rm c} > 700 \, {\rm km \, s^{-1}}$. We report these results at four different redshifts $z = 0.0, 0.25, 0.5$ and 10.

We find that a fraction of 50%-60% of the halos in the group sample present displacement equal or larger than the observed displacement for SL2S J08544-0121. For halos in the cluster sample this fraction increases to 80%-85%.

We also describe the collision geometry by the angle between the position and velocity vectors of the sub-halo with respect to the host. This allows us to separate three different instances: the sub-halo crossing the host virial radius, the sub-halo going through the host's center and the secondary infall after reaching apogee.

From this analysis we derive an estimate for the displacement between the DM and the baryonic component. In the group sample 0.1%-1.0% of the halos show a displacement equal or larger than the measurements of SL2S J08544-0121by (Gastaldello et al. 2014). In the cluster sample this fraction rises to 4%-10%.

The results we present here can be used as a potential test of ΛCDM. [...]

The CosmoSim database used in this paper is a service by the Leibniz-Institute for Astrophysics Potsdam (AIP). The BolshoiP simulation was performed within the Bolshoi project of the University of California High-Performance AstroComputing Center (UC-HIPACC) and was run at the NASA Ames Research Center.

REFERENCES

Bradač, M., Allen, S. W., Treu, T., Ebeling, H., Massey, R., Morris, R. G., von der Linden, A., & Applegate, D. 2008, ApJ, 687, 959
Bryan, G. L., & Norman, M. L. 1998, ApJ, 495, 80
Clowe, D., Bradač, M., Gonzalez, A. H., Markevitch, M., Randall, S. W., Jones, C., & Zaritsky, D. 2006, ApJ, 648, L109

Dahle, H., Sarazin, C. L., Lopez, L. A., Kouveliotou, C., Patel, S. K., Rol, E., van der Horst, A. J., Fynbo, J., Wijers, R. A. M. J., Burrows, D. N., Gehrels, N., Grupe, D., Ramirez-Ruiz, E., & Michałowski, M. J. 2013, ApJ, 772, 23
Dawson, W. A., Wittman, D., Jee, M. J., Gee, P., Hughes, J. P., Tyson, J. A., Schmidt, S., Thorman, P., Bradač, M., Miyazaki, S., Lemaux, B., Utsumi, Y., & Margoniner, V. E. 2012, ApJ, 747, L42

Farrar, G. R., & Rosen, R. A. 2007, Physical Review Letters, 98, 171302

Forero-Romero, J. E., Gottlöber, S., & Yepes, G. 2010, ApJ, 725, 598

Gastaldello, F., Limousin, M., & Foex, G. 2014, MNRAS submitted

Hayashi, E., & White, S. D. M. 2006, MNRAS, 370, L38

Hinshaw, G., Larson, D., Komatsu, E., Spergel, D. N., Bennett, C. L., Dunkley, J., Nolta, M. R., Halpern, M., Hill, R. S., Odegard, N., Page, L., Smith, K. M., Weiland, J. L., Gold, B., Jarosik, N., Kogut, A., Limon, M., Meyer, S. S., Tucker, G. S., Wollack, E., & Wright, E. L. 2013, ApJS, 208, 19

Klypin, A., Gottlöber, S., Kravtsov, A. V., & Khokhlov, A. M. 1999, ApJ, 516, 530

Klypin, A., & Holtzman, J. 1997, ArXiv Astrophysics e-prints

Klypin, A. A., Trujillo-Gomez, S., & Primack, J. 2011, ApJ, 740, 102

Lee, J., & Baldi, M. 2012, ApJ, 747, 45

Lee, J., & Komatsu, E. 2010, ApJ, 718, 60

Markevitch, M., Gonzalez, A. H., Clowe, D., Vikhlinin, A., Forman, W., Jones, C., Murray, S., & Tucker, W. 2004, ApJ, 606, 819

Merten, J., Coe, D., Dupke, R., Massey, R., Zitrin, A., Cypriano, E. S., Okabe, N., Frye, B., Braglia, F. G., Jiménez-Teja, Y., Benítez, N., Broadhurst, T., Rhodes, J., Meneghetti, M., Moustakas, L. A., Sodré, Jr., L., Krick, J., & Bregman, J. N. 2011, MNRAS, 417, 333

Muñoz, R. P., Motta, V., Verdugo, T., Garrido, F., Limousin, M., Padilla, N., Foëx, G., Cabanac, R., Gavazzi, R., Barrientos, L. F., & Richard, J. 2013, A&A, 552, A80

Riebe, K., Partl, A. M., Enke, H., Forero-Romero, J., Gottlöber, S., Klypin, A., Lemson, G., Prada, F., Primack, J. R., Steinmetz, M., & Turchaninov, V. 2013, Astronomische Nachrichten, 334, 691

Springel, V., & Farrar, G. R. 2007, MNRAS, 380, 911

Thompson, R., & Nagamine, K. 2012, MNRAS, 419, 3560